Polymer 49 (2008) 5215–5224

Contents lists available at ScienceDirect

Polymer

journal homepage: www.elsevier.com/locate/polymer

Study of the organic–inorganic phase interactions in polyester–titania hybrids

Laura Mazzocchetti [a], Mariastella Scandola [a,*], Antonino Pollicino [b]

[a] Dipartimento di Chimica "G. Ciamician", Università di Bologna and INSTM UdR Bologna, Via Selmi 2, 40126 Bologna, Italy
[b] Dipartimento di Metodologie Fisiche e Chimiche per l'Ingegneria, Università di Catania and INSTM UdR Catania, Viale A. Doria 6, 95125 Catania, Italy

ARTICLE INFO

Article history:
Received 27 June 2008
Received in revised form 29 August 2008
Accepted 11 September 2008
Available online 27 September 2008

Dedicated to the memory of the scientist and friend Prof. Zbigniew Jedlinski.

Keywords:
Organic–inorganic hybrid
Titania
Polyester

ABSTRACT

Radiopaque organic–inorganic hybrids were prepared by the sol–gel procedure. The hybrid the organic phase is a polyester, poly(1,4-butyleneglutarate), while the inorganic domains are *in situ* synthesized titania. FT-IR and XPS analyses show that organic and inorganic phases strongly interact mainly because of transesterification reactions involving the polyester chain and Ti atoms during hybrid synthesis. Synthetic parameters, namely solvent, environment acidity and inorganic precursor content, are investigated in order to assess their influence on the solid-state behaviour of the hybrid. The ability of the solvent to solvate, but not complex, Ti atoms and the presence of an inorganic acid in the feed increase interaction between the organic and inorganic phases, thus hindering polymer chain mobility. A similar effect, outlined by T_g increase and crystallization inhibition, is induced by increasing inorganic phase content. All obtained hybrids are optically transparent and opaque to X-rays.

1. Introduction

Hybrid materials, also named ceramers, represent the natural interface between two traditionally far away worlds: organic chemistry and inorganic chemistry. This fairly new class of materials, whose first examples date back to the eighties [1,2], may take advantage from characteristic properties of both organics and inorganics, such as high ductility and low temperature processing conditions typical of polymers and high modulus, thermal stability and low coefficient of thermal expansion distinctive of inorganic materials. Moreover, organic–inorganic hybrids may display synergistic properties with respect to the bare sum of the plain components' features, such as remarkable improvements in mechanical [3], thermal [4,5], electrical [6], and magnetic [7] properties. In particular, the nano-structured morphology of the inorganic domains strongly affects the physical behaviour of the hybrids leading to interesting properties such as, among others, optical transparency [8]. Due to the wide range of applicability fields of this class of materials, a number of hybrids are already commercially available [9].

A wide spectrum of polymers are employed as the organic phase constituent of ceramers: polydimethylsiloxane (PDMS), used in the first reported ceramer [1,10–12], poly(tetramethylene oxide) (PTMO) [12–15], polycaprolactone (PCL) [16–18], polyoxazoline [19], poly(ether ketone) [20], polyethylene oxide [21], etc. The hybrid inorganic phase is usually a metal oxide. Although many oxides are reported in the literature, such as those of titanium, zirconium, aluminium or cerium, silicon oxide (silica) is definitely the most widely applied in ceramers [22], owing to the easiness of its preparation. However, in recent years, titania has gained increasing interest as inorganic component for hybrid production [23,24], owing to its peculiar properties (i.e. X-rays and UV-radiation absorption, high refractive index, photocatalytic properties) that can lead to new functional organic–inorganic materials.

The most common way to synthesize a metal oxide is the sol–gel procedure that, starting from transition metal alkoxides (TMA), via a complex sequence of hydrolysis and condensation reactions, leads to the inorganic network [25]. This synthetic methodology is well known in the literature regarding plain metal oxide production [26] and it can be successfully transferred to the synthesis of organic–inorganic hybrids [27]. In particular if the sol–gel procedure is carried out using a suitable TMA in the presence of a polymer bearing functional groups able to covalently bind to the metal oxide network, in the resulting hybrid the organic and inorganic phases will be connected through chemical bonds. An interesting feature of the sol–gel technique is the mild working condition employed, i.e. low temperature, that prevents undesired thermal degradation of the polymer.

Hybrids containing titania as the inorganic component are interesting radiopaque and UV-blocking materials [28]. The sol–gel technique allows an easy '*in situ*' synthesis of the hybrid in the form of a thin coating layer that can be applied in the medical field for traceability of medical devices.

* Corresponding author. Tel.: +39 051 2099577; fax: +39 051 2099456.
E-mail address: mariastella.scandola@unibo.it (M. Scandola).

0032-3861/$ – see front matter © 2008 Elsevier Ltd. All rights reserved.
doi:10.1016/j.polymer.2008.09.029

In this context, recent literature concerning biomaterials for surgical and prosthetic applications outlines the need to develop new materials that allow easy detection of device position by fluoroscopy or X-ray radiography [29,30]. At present several strategies are adopted to improve traceability of medical devices. A first approach, used for the production of new intrinsically traceable devices that yield a contrasted image against the background of a fluoroscope or X-ray film, is based on a suitable modification of the bulk material, as proposed by Jayakrishnan et al. [31–33]. They blended polymers such as poly(hydroxyethylmethacrylated) P(HEMA), polyurethanes and poly(vinyl alcohol) with "markers" that block the transmission of X-rays, such as barium sulphate or tantalum particles. An alternative route was followed by Cabasso et al. [34,35], who produced polymer–salt complexes by dissolution of a radiopaque heavy metal salt (i.e. bismuth bromide or uranyl nitrate) in the monomer, which was subsequently polymerized. In addition, many authors proposed the synthesis of intrinsically radiopaque polymers either by co-polymerization of vinyl monomers (i.e. barium or zinc acrylates) [36] or by grafting iodine-containing molecules onto preformed high molecular weight polymers [37–40]. Although all the reported materials are able to give a clearly contrasted radiographic image, the procedure used to impart radiopacity may induce changes in the bulk properties of the polymeric material that negatively affect device performance. An alternative approach consists in coating the surface of the medical device with a thin layer of a radiopaque material (typically heavy metal salts, plain metals, etc.). In this way the impact of the radiopacifying agent on the device bulk properties is drastically reduced. However, the procedures reported in the literature for coating application require either rather complex deposition technologies [41,42] or high temperature conditions [43] unsuitable for polymeric materials. A smart solution to the traceability problem of polymeric devices may be provided by the use of a radiopaque hybrid coating, synthesized and applied by facile techniques [28].

This work reports the synthesis and characterization of radiopaque organic–inorganic hybrids composed of poly(1,4-butyleneglutarate) (PBG) and titanium oxide (titania). With the aim of understanding and controlling physical and structural properties of the ceramers, different synthetic conditions (i.e. solvent type, acid concentration, relative amount of organic and inorganic precursors in the feed) are investigated to assess their influence on the final hybrid behaviour.

2. Experimental section

2.1. Materials

THF (Riedel de Han), chloroform (Aldrich), poly[1,4-butyleneglycol] $\overline{M}_n = 1000$ (PBG, Aldrich), titanium tetraisopropoxide (TIPT, Aldrich) and concentrated hydrochloric acid (37%) (HCl, Aldrich) were used without further purification.

2.2. Hybrid synthesis

The precursors of the hybrid organic and inorganic phases, PBG and TIPT respectively, are dissolved in different weight ratios (75/25, 50/50, 40/60 and 25/75 w/w) in the solvent (1 g of PBG + TITP in 3 ml of THF or of $CHCl_3$). HCl is added in some cases (10/100, 20/100 or 30/100 HCl/TIPT molar ratios). The hybrids are labelled T*X*-*Y* and C*X*-*Y*, where T and C indicate the solvent (THF or chloroform), label X represents the weight percentage of inorganic phase precursor TIPT in the sol–gel feed (25, 50, 60 or 75), and Y indicates the HCl/TIPT percentage molar ratio (0, 10, 20, 30).

A representative synthesis is as follows: 1.0 g TIPT is added to 2 ml of solvent (THF or $CHCl_3$), then HCl (70 μl, 20 mol% HCl/TIPT) is added under vigorous stirring at ambient temperature (solution 1). In a separate container 1.0 g PBG is dissolved in 4 ml of the same solvent (solution 2). After complete polymer dissolution, solution 2 was added to solution 1 under vigorous stirring. The obtained clear solution is then cast in a Teflon coated container and covered with a glass lid in order to slow the sol–gel process rate. After 22 h at room temperature, a solid transparent material is recovered, which is thermally treated for 2 h in an oven at 110 °C.

For the sake of comparison, the plain inorganic component (i.e. titania) is also produced following the same synthetic pathway described above for hybrid synthesis, without addition of solution 2.

2.3. Characterization techniques

Thermogravimetric (TGA) measurements are carried out using a TA-TGA 2950. The analyses are performed at 10 °C/min from room temperature to 600 °C under air flow (60 ml/min).

Differential Scanning Calorimetric (DSC) measurements are performed using a TA DSC-Q100 apparatus, equipped with an LNCS (Liquid Nitrogen Cooling System) accessory. Samples (about 5 mg) are placed in Al pans and are subjected to 3 subsequent heating runs at 20°/min from −100 °C up to 100 °C. Controlled cooling at 10°/min is applied after the first heating scan, while quench cooling is performed after second heating scan. T_g values are taken at half-height of the glass transition heat capacity step.

Infrared spectra are recorded on a Nicolet 380 FT-IR, with 32 scans and 4 cm^{-1} resolution. Samples are dried overnight in a desiccator over P_2O_5 before measurement. Solid insoluble samples are ground with KBr (1 mg sample/100 mg KBr) and pelletized under pressure. Analysis of the starting polymer (PBG) is performed by dissolving it in a small amount of chloroform and casting a few drops of solution on a KBr disc, allowing solvent evaporation prior to measurement.

The XPS measurements are carried out by a VG instrument electron spectrometer using a $MgK_{\alpha 1,2}$ X-ray source (1253.6 eV). The X-ray source in the standard conditions works at 100 W, 10 kV and 10 mA. The base pressure of the instrument is 5×10^{-10} Torr and the operating pressure typically is 2×10^{-8} Torr. A pass energy of 100 eV and 50 eV is used for wide scans and narrow scans respectively. Measurements are carried out on electrons taking-off (t.o.a.) from sample surface with an angle of 45°. All data analyses (linear background subtraction and peak integration) are accomplished using a VGX900x (version 6) software. Binding energies are referenced to the C–H level at 285.0 eV.

Radiographic images of the hybrids are recorded on a mammographic apparatus (Diamond MGX, Instrumentarium Co. Imaging Division) equipped with a radiogenic tube Varian M113SP. The experimental parameters are: 22 keV, 4 mA/s and 21 cm sample-to-detector distance.

3. Results and discussion

All hybrids investigated in the present work are prepared via sol–gel method. It is well known that the sol–gel process implies hydrolysis and condensation reactions (Scheme 1). Water plays a key role in the process, allowing hydrolysis of the alkoxide groups to form intermediate metal hydroxides (reaction 1) which can then condensate to produce the metal oxide network (reactions 2 and 3). It is well known that TMAs are very reactive towards nucleophilic reagents, such as water [25]. This high reactivity results from low electronegativity of the metal, and from the possibility of transition metals to expand their coordination number [44]. In typical sol–gel reactions using TMA in the presence of water, instantaneous precipitation of a solid, the metal oxide, is commonly observed. Therefore, in view of the fact that the TMA used in this work (TIPT) is a highly hydrolysable precursor, no water is added to the hybrid

The sol-gel Process

Hydrolysis:

$$M(OR)_n + H_2O \rightarrow M(OR)_{n-1}(OH) + ROH \quad [1]$$

Condensation:

$$M(OR)_n + M(OR)_{n-1}(OH) \rightarrow (RO)_{n-1}M\text{-}O\text{-}M(OR)_{n-1} + ROH \quad [2]$$

$$M(OR)_{n-1}(OH) + M(OR)_{n-1}(OH) \rightarrow (RO)_{n-1}M\text{-}O\text{-}M(OR)_{n-1} + H_2O \quad [3]$$

Scheme 1.

reaction mixture, and, as earlier reported [45], it is assumed that air humidity is enough to promote alkoxide hydrolysis.

The organic phase precursor is a viscous low molecular weight di-hydroxy terminated polyester (PBG $\overline{M}_n$ = 1000 Da), whose OH functionalities may interact with titanium alkoxide (TIPT) during sol–gel process. After room temperature gelation (22 h) all obtained samples, irrespective of feed composition and of solvent, are transparent solids. A thermal treatment (2 h at 110 °C) is additionally applied in order to push forward reactions and induce volatilization of reaction by-products [46].

3.1. Effect of the sol–gel solvent

In order to investigate the solvent effect on the final hybrid properties, the synthesis reaction is carried out both in THF and in chloroform that are good solvents for all reactants. In fact, while chloroform cannot interact with the transition metal, THF might be able to complex titanium via its ether oxygen [47].

The effect of the solvent on hybrid synthesis is exemplified below in the case of samples produced from a given TIPT/PBG feed ratio (50:50), using either THF or chloroform. In neither case acid is added, hence the hybrids are labelled T50-0 and C50-0 respectively. After room temperature gelation and further thermal treatment the obtained materials are analyzed by TGA. For the sake of comparison the thermogravimetric behaviour of the starting polymeric precursor (PBG) is also analyzed. Fig. 1 compares the TGA curves in air of the mentioned samples. PBG starts loosing weight above 240 °C, and degrades in a multistep process that leads to an almost negligible residue above 550 °C. Thermal degradation of both hybrids proceeds via a multistep process that starts at a temperature 50–70 °C lower than that of the plain polymer. The observed lower thermal stability of the hybrids might be due to degradation

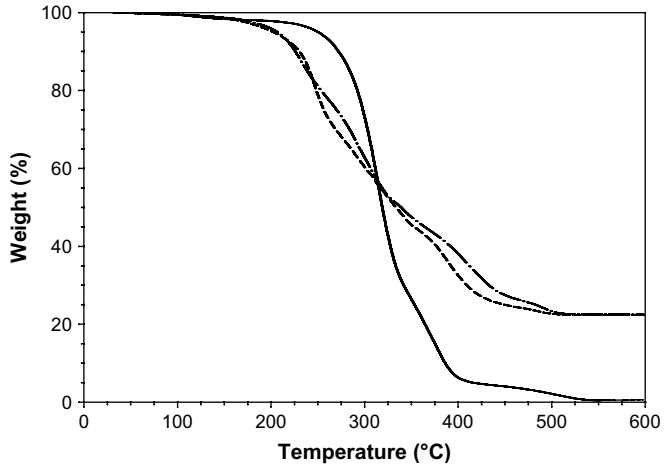

Fig. 1. TGA curves in air of PBG $\overline{M}_n$ = 1000 Da (—) and of hybrids T50-0 (- - -) and C50-0 (— - —).

reactions involving titanium oxide, that is a well known catalyst [48–50]. Thermal degradation of both hybrids in Fig. 1 ends around 550 °C, leaving a consistent solid residue. Since the organic polymer is completely degraded at 600 °C, the residue at the end of the heating scan, whose value for both hybrids is listed in Table 1, is attributed to the inorganic component of the material.

The TGA measurements are carried out in air, hence all carbon-based compounds are oxidized and volatilize during the scan while titanium atoms, independent of their initial oxidation state, end up as fully oxidized, i.e. as titanium oxide. The solid residue measured after hybrid thermal degradation may thus reveal the amount of Ti atoms present in the starting material and consequently it yields useful information about the actual composition of the analyzed material. For a given hybrid, the theoretical amount of titania solid residue ($SR^A_{TiO_2}$) expected at the end of a TGA scan such as those in Fig. 1 can be calculated, on the assumption that during the sol–gel process complete hydrolysis and condensation of the inorganic phase precursor have occurred. For example, for the hybrid synthesized from a mixture of PBG and TIPT in a 50/50 wt% ratio $SR^A_{TiO_2}$ is given by the following equation:

$$SR^A_{TiO_2} = \frac{X_{TIPT}\dfrac{MW_{TiO_2}}{MW_{TIPT}}}{X_{PBG} + X_{TIPT}\dfrac{MW_{TiO_2}}{MW_{TIPT}}}, \quad (1)$$

where X_{PBG} and X_{TIPT} are the weight fractions of the organic and inorganic precursors in the feed and MW_{TiO_2} and MW_{TIPT} are the molecular weights of titania and of TIPT respectively. Comparison of the experimental solid residues for the two hybrids obtained in THF and in chloroform with the calculated data, also reported in Table 1, shows good agreement. This observation suggests that prior to thermogravimetric analysis almost complete hydrolysis of the inorganic precursor has occurred in the hybrid. Sol–gel of TMAs is usually an equilibrium process, driven by several parameters affecting the relative rates of hydrolysis and condensation, that does not reach completeness at RT [44,51,52]. Under thermal treatment, the Ti–OR and Ti–OH groups still present after RT ageing can further react releasing ROH and H_2O, both via sol–gel reactions and involving the reactive functionalities of highly mobile PBG chains. The TGA results show that upon curing at 110 °C the hydrolysis reaction is almost complete and the reaction by-products are eliminated.

With the aim of investigating the solvent effect on the mobility and on the phase behaviour (amorphous/crystalline) of the polymeric hybrid component, the T50-0 and C50-0 samples are also analyzed by DSC (Fig. 2 and Table 1). For the sake of comparison, Fig. 2 also displays the DSC curve of the polymeric precursor PBG that shows a stepwise specific heat increment (T_g = −72 °C) followed by a cold crystallization exotherm and by a multiple melting endotherm. Conversely, the only feature in the DSC curves of both hybrids is the glass transition, located at higher temperature with respect to that of plain PBG (see magnified inset in Fig. 2). In the

Table 1
Solvent effect on thermal properties of hybrids

Sample	Feed	Titania residue		DSC[a]				
	TIPT/PBG (wt%)	Exp.[b] (%)	Calc.[c] (%)	T_g (°C)	ΔT_g (°C)	ΔCp (J/g °C)	T_m (°C)	ΔH_m (J/g)
PBG	–	<0.5	0	−72	8	0.68	13	44
T50-0	50/50	22.4	21.9	−69	10	0.40	–	–
C50-0	50/50	22.5	21.9	−61	12	0.40	–	–

[a] From second heating scan after quench cooling.
[b] Experimental solid residue at 600 °C evaluated from TGA experiments run in air.
[c] Calculated according to Eq. (1), on the assumption that the hybrid precursors have fully reacted before TGA scan.

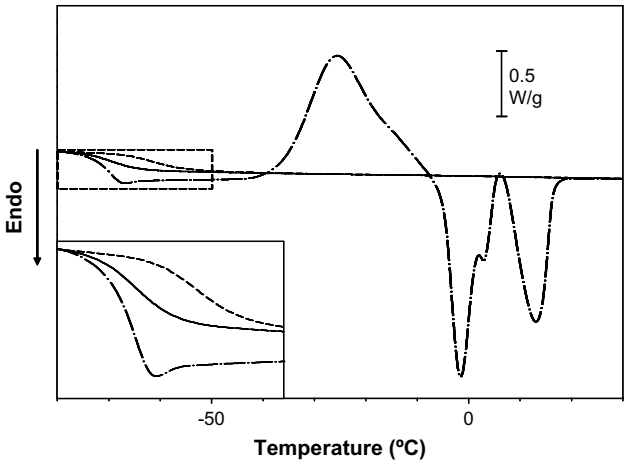

Fig. 2. DSC curves (2nd scan after quench cooling) of PBG (— - —) and of hybrids T50-0 (——) and C50-0 (- - -). Inset: focus on the glass transition region.

hybrids polymer crystallization is completely prevented. The DSC behaviour suggests that in the hybrids the organic PBG phase strongly interacts with titania, that limits PBG chain mobility both by increasing T_g and by hindering the molecular rearrangements leading to crystallization. This result is consistent with earlier work by the authors on silica-based hybrids [46,53] and shows that the hindrance to polymer mobility in the present samples is higher when using chloroform instead of THF as the solvent in the sol–gel reaction (see higher T_g value of C50-0 in Table 1).

In order to get an insight into the interactions between PBG and titania in the hybrids, the FT-IR technique is applied. Fig. 3 compares the infrared spectra of the two hybrids (T50-0 and C50-0) with those of plain PBG and of titania. The metal oxide is synthesized by the sol–gel method, in the same experimental conditions applied for hybrid production except for omission of polymer addition step. The titania curve shown in Fig. 3 refers to a sample synthesized in THF solution. No significant difference is observed in the FT-IR spectrum of titania obtained from chloroform solution, hence the titania curve in Fig. 3 is a fair reference for both hybrids.

The infrared spectrum of titania does not show the well defined absorption bands typical of the crystalline titanium dioxide polymorphs (anatase, rutile, etc.) being, instead, in close agreement with the literature spectrum for completely amorphous TiO_2 [54]. This is an expected result, owing to the low temperature (110 °C) and short time (2 h) of the heat treatment applied to the material, which is not expected to promote crystal phase formation [55,56]. The most prominent features in the TiO_2 spectrum are: (a) the wide OH stretching region centred at 3000 cm^{-1} and spanning over 1000 cm^{-1}, where the vibrations of Ti–OH and of absorbed water appear, and (b) the broad absorption region ranging from 400 to 1000 cm^{-1} that is typical of Ti–O–Ti vibrations of amorphous titanium oxide [54,57]. In the polyester spectrum, as expected, the most intense band is that of carbonyl stretching at 1735 cm^{-1}. A small absorption around 3500 cm^{-1} accounts for the hydroxyl terminal moieties of the polymer. It is worth noting that in the polymer spectrum no significant signal appears below 900 cm^{-1}, i.e. in the Ti–O–Ti spectral region.

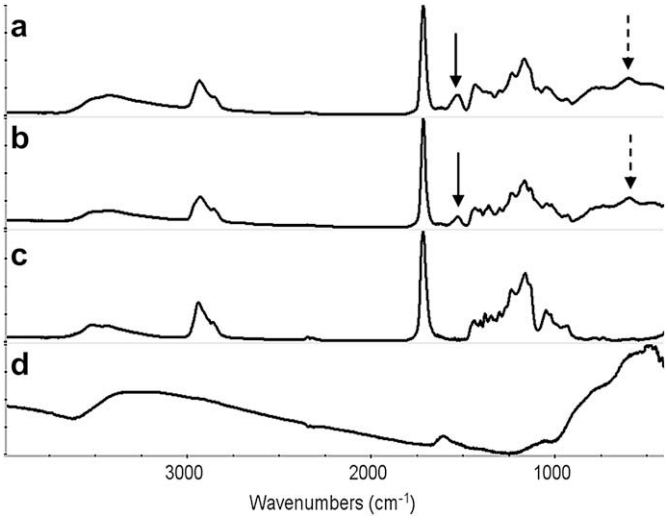

Fig. 3. Normalized FT-IR spectra of: (a) C50-0, (b) T50-0, (c) PBG and (d) titania. Solid arrow: band at 1535 cm^{-1}; broken arrow: band at 610 cm^{-1}.

The two hybrids in Fig. 3 show the characteristic absorption bands of PBG, together with those typical of the titania component (400–1000 cm^{-1}). Among the TiO_2 related vibrations, particularly prominent in the hybrids with respect to its intensity in plain titania is the band at 610 cm^{-1} (broken arrow in Fig. 3). Worth noting in both hybrid spectra is a new band around 1535 cm^{-1} (solid arrow in Fig. 3), absent in both PBG and TiO_2 spectra.

Extensive studies, mainly focused on low molecular weight substances, have been carried out to investigate the vibrational absorptions of organometallic compounds. In organotitanium products, Adams [26] reported an absorption in the region from 580 to 610 cm^{-1} that they attributed to the Ti–O vibration in compounds where the oxygen atom is linked to an organic residue. This assignment was further confirmed by Hampden-Smith et al. [58] who reported that the band frequency shifts when the organic moiety is fully deuterated. In the present hybrids, residual titanium alkoxide groups from the sol–gel process have been ruled out by the TGA results discussed above. Hence, according to the mentioned literature assignments, the absorption at 610 cm^{-1} (Fig. 3) is attributed to the Ti–O stretching vibration of Ti–O–C groups, formed by covalent bonding of PBG chain with the TiO_2 network.

As concerns the band appearing in the hybrid spectra around 1535 cm^{-1}, Takahashi et al. [45] reported an absorption at the same frequency in a complex between stearic acid and TiO_2. This band was attributed to carbonyl stretching of the stearic acid C═O moiety interacting with the titanium atom, being well known that a carbonyl group complexing an electron-deficient atom shifts its absorption to lower wavenumbers to an extent which depends on the mode of interaction [59]. Hence in the present hybrids, the absorption at 1535 cm^{-1} is assigned to carbonyl groups of the polyester chain interacting with titanium via oxygen atom to fulfil metal electron-deficiency. In particular, the wavelength of the absorption seems to be in good agreement with values reported in the literature for a bidentate carboxylate group [23,59]. The presence of such functionality in the hybrid may find its reason in transesterification of polyester chain, as sketched in Scheme 2. This reaction is well known to be promoted by the presence of a Lewis acid, such as Ti atoms. Although it is clear, from the frequency shift, that a bidentate structure is formed, at present it is not possible to distinguish between a bidentate chelating carboxyl and a bidentate bridging one (see structures proposed in Scheme 2). The FT-IR results indicate that PBG and Ti are thus able to interact not only via the reactive hydroxylic chain ends forming covalent bonds during sol–gel, but also by complexing interactions of carboxyl oxygens with Ti atoms. These reactions, involving polymer hydroxyls and/or caboxylates and Ti atoms, are known to be fast and have been already reported in the literature [60–62].

It is worth noting that the intensity of the 1535 cm^{-1} absorption in the spectra of Fig. 3 is stronger when chloroform instead of THF is used in the sol–gel procedure. A possible explanation of the

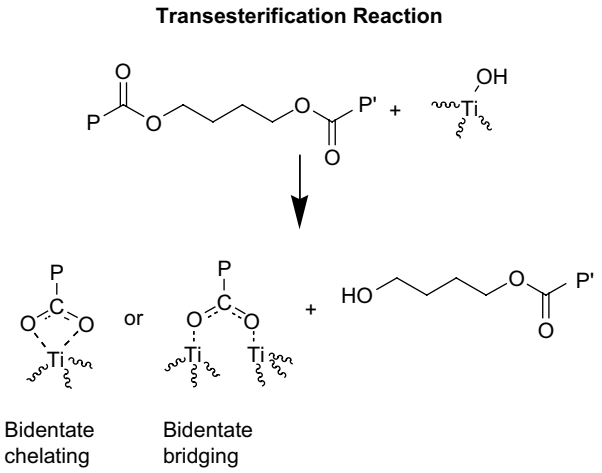

Scheme 2.

observed behaviour may be the ability of THF oxygen to compete with the polyester carbonyls for titanium interaction, thus shielding the Lewis acid centre and hindering the transesterification activity [47]. On the contrary, no such interaction can be reasonably expected with chloroform. Hence, a larger interaction between the polyester carbonyls and titania occurs when the hybrid is prepared in chloroform. It is interesting to note that the effects of THF "complexation" in solution persist after complete solvent removal, at the end of the hybrid preparation procedure. This result suggests that the covalent and complexing interactions between organic and inorganic phases occurring in the presence of the solvent somehow lock in the polymer chain, preventing further significant rearrangements upon solvent evaporation. Worth noting is the fact that THF is more hydrophilic than $CHCl_3$ and that water absorbed by both solvents from the environment should accelerate hydrolysis rate and favour polymer–Ti interactions. On the contrary, the present results show that in THF – where the water content should be higher – the organic–inorganic network is looser. This result highlights the importance of the suggested THF–Ti complexing interactions and the minor effect played by absorbed water on the overall hybrid behaviour.

The proposed interaction model explains not only the FT-IR results, but also the solvent effect on the hybrid T_g (Table 1). In fact, the higher extent of interaction between PBG and titania in $CHCl_3$ leads to lower chain mobility and, consequently, to higher T_g of C50-0 than T50-0.

3.2. Effect of acid addition during sol–gel

Among the aims of this work is the investigation of the influence of acid addition during hybrid synthesis. It is well established that TMAs quickly undergo hydrolysis and condensation, resulting in uncontrolled fast precipitation of the oxide [63]. The presence of an inorganic acid, that is commonly applied in the synthesis of plain titania by sol–gel [64], is intended to modify the relative rate of the hydrolysis and condensation reactions, by favouring the former process and slowing down the latter. Alternatively, instead of using H^+, some chelating agents may be added to the alkoxide solution before sol–gel reaction with the aim of reducing metal atom reactivity [25].

In ceramer synthesis the addition of a chelating agent bears as a consequence the presence of a third party that may interfere in the hybrid production process. When hybrids for specific applications are synthesized, such as, for example, materials to be applied in the medical field, the use of potentially harmful components should be avoided or – at least – such substances should be totally and safely removed from the biomaterial after synthesis. Such a post-fabrication procedure cannot be satisfactorily applied to highly cross-linked solid materials such as the ceramers. Hence, in this work the use of chelating molecules is discarded and hydrochloric acid is selected to slow down the condensation reaction rate [64]. The properties of hybrids synthesized in the presence or absence of HCl are compared. The proton cation is expected to accelerate hydrolysis reaction, thus providing longer life to titanium hydroxide groups before condensation. Early TiO_2 precipitation is disfavoured and the probability of reaction between the polymer chains and titanium hydroxide increases (note that acid is added to TIPT sol, before addition of polymer solution, see Section 2). The acidic reaction environment also influences the reactivity of polymer chain. In fact transesterification (Scheme 2) is favoured by the presence of H^+ that catalyzes polyester chain reaction, thus promoting interactions between carboxylic moiety and Ti atoms.

Hybrid (50:50 TIPT/PBG) has been synthesized using different HCl contents and two hybrid series are analyzed, one synthesized in THF, the other in chloroform, labelled T50-*Y* and C50-*Y*, where *Y* indicates the HCl/TIPT percentage molar ratio in the feed. TGA experiments on the hybrids lead to curves (not shown) similar to those reported in Fig. 1 for samples obtained without acid addition. In all cases, a consistent solid residue at 600 °C is found (Table 2), whose value satisfactorily compares with that (21.9%) calculated for the completely reacted 50:50 feed, already reported in Table 1 and discussed above. This result confirms that the adopted preparation procedure drives the TIPT hydrolysis reactions to completion and fully removes reaction by-products.

Table 2 reports the results of DSC measurements carried out on the two hybrid series. Irrespective of the acid content and unlike plain PBG, the ceramers show no crystallization/melting phenomena. All hybrids show a glass transition, whose temperature seems to increase with increasing acid amount in the feed, both in THF and in chloroform. The remaining glass transition parameters, i.e. width (ΔT_g) and intensity (ΔCp), do not differ substantially. As an example, Fig. 4 shows the effect of acid content on the DSC curves of the T50-*Y* series ($Y = 0$, 10, 20, 30). With increasing amount of H^+ in the feed up to 20 mol% (H^+/Ti), T_g increases, while higher H^+ concentrations seem not to influence the glass transition any more. Similar curves (not shown) are obtained for the C50-*Y* series.

As mentioned in the literature [63], the presence of H^+ in the sol–gel feed should slow down condensation rate, thus keeping the metal moiety hydrolyzed for a longer time. In this circumstance all kinds of polymer–Ti interactions are favoured. As a consequence, the higher is the H^+ content in the mixture, the stronger is the interaction between polymer and titania, that results in an increase of T_g.

It must be pointed out that adding increasing amounts of HCl 37% in the reaction mixture implies a concomitant water content increase. Consequently the initial hydrolysis ratio H ($H = [H_2O]/[Ti]$), that is one of the key parameters affecting the final structure of the forming titanium oxide [52], changes. Sanchez and coworkers [25,44,51,52] have thoroughly demonstrated that when $H < 1$, such as in the present conditions, hydrolysis and formation of small titanium oxo-organo clusters are favoured. These small entities with a large number of hydrolyzed Ti–OH groups may easily interact with PBG, leading to the formation of the organic–inorganic network. Hence, both H^+ and the water solvent act in the same direction, so that it cannot be excluded that the above discussed acid effect might result from the concurring action of both parameters.

Table 2 shows that T_g does not change when the H^+ content varies from 20% to 30% in neither hybrid series. The presence of a threshold T_g value seems to suggest that acid increment above

Table 2
Effect of the presence of acid on hybrid thermal properties

Sample	Feed		TGA[a]			DSC[b]		
	TIPT/PBG (wt%)	HCl/Ti[c] (mol%)	Residue (%)	T_g (°C)	ΔT_g (°C)	ΔCp (J/g °C)	T_m (°C)	ΔH_m (J/g)
PBG	–	–	<0.5	−72	8	0.68	13	44
T50-0	50/50	0	22.4	−69	10	0.40	–	–
T50-10	50/50	10	21.7	−65	12	0.42	–	–
T50-20	50/50	20	22.1	−57	16	0.45	–	–
T50-30	50/50	30	22.4	−57	13	0.39	–	–
C50-0	50/50	0	22.5	−61	12	0.40	–	–
C50-10	50/50	10	23.3	−61	12	0.35	–	–
C50-20	50/50	20	21.1	−54	11	0.39	–	–
C50-30	50/50	30	22.0	−54	11	0.37	–	–

[a] Experimental solid residue at 600 °C.
[b] From second heating scan after quench cooling.
[c] Molar ratio of acid vs. titanium (in titania precursor TIPT).

20% is unable to promote additional polymer–titania interactions and to further limit polymer mobility.

As already observed in the absence of acid, the glass transition temperatures of samples with the same acid feed are higher when chloroform is used as solvent, confirming the proposed competition between THF and polymer for Ti interaction.

FT-IR spectroscopy applied to both T50-Y and C50-Y series yield spectra (not shown) very similar to those reported in Fig. 3. No effect of acid addition in the concentration range explored is detected by this technique.

3.3. Effect of inorganic phase content

With the aim of assessing the effect of the inorganic phase content on material properties, hybrids with different feed compositions (TIPT/PBG = 25/75, 50/50, 60/40 and 75/25 by weight) are prepared in both THF and chloroform solutions. They are all synthesized with HCl/Ti 20 mol%, i.e. the acid amount that yields the threshold (highest) T_g value in both T50-*Y* and C50-*Y* series discussed above. The new samples are labelled T*X*-20 and C*X*-20, where *X* is the TIPT content in the feed, expressed in weight percentage.

TGA measurements show that thermal degradation proceeds through several steps and ends, as expected, with a solid residue that increases with the amount of inorganic phase precursor in the feed (Table 3). It is worth mentioning that in principle unwanted organic products might be present in the material, owing to incomplete reaction of metal alkoxides during hybrid synthesis and/or to inefficient volatilization of reaction by-products (for example the alcohol produced from metal alkoxide hydrolysis).

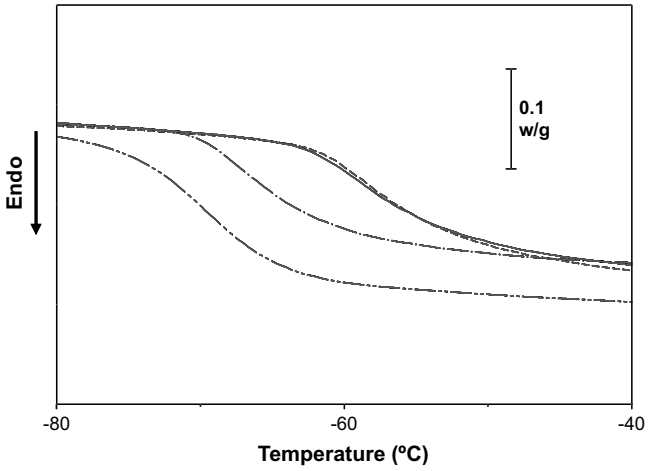

Fig. 4. DSC curves of T50-*X* hybrids, focused in the T_g region: T50-0 (— - - —), T50-10 (— - —), T50-20 (- - -) and T50-30 (——).

As already discussed for hybrids C-50Y and T50-Y, TGA can help understanding if the TIPT hydrolysis has run to completion, through the analysis of the final solid residue. The TGA residue at 600 °C of the synthesized hybrids (Table 3) can thus be compared with two limit situations, as illustrated in Fig. 5 for the CX-20 series. One limit case stands on the assumption that the sample is a hybrid composed of titania and polymer only, i.e. a hybrid resulting from sol–gel reaction pushed to completion with total elimination of reaction by-products. In this case, the theoretical solid residue ($SR^A_{TiO_2}$) is calculated using Eq. (1) illustrated above. In the second limit case, the theoretical solid residue is calculated as if a completely unreacted TIPT and PBG mixture were thermally degraded during the TGA scan in air purge. In this circumstance PBG is not the only organic component that can thermally degrade upon heating, because the alkoxide groups belonging to TIPT can also be oxidized. In this case the solid residue ($SR^B_{TiO_2}$) is calculated according to the following equation:

$$SR^B_{TiO_2} = \frac{X_{TIPT}\frac{MW_{TiO_2}}{MW_{TIPT}}}{X_{PBG} + X_{TIPT}}, \quad (2)$$

where X_{PBG} and X_{TIPT} are weight fractions of organic and inorganic precursors in the feed and MW_{TiO_2} and MW_{TIPT} are molecular weights of titania and TIPT respectively.

Fig. 5 compares the experimental solid residue of four hybrids of the CX-20 series with different TIPT weight fractions (X_{TIPT}) in the feed with the behaviours predicted by Eqs. (1) and (2) discussed above. An excellent agreement between experimental values and the prediction of Eq. (1) is observed. This result shows that all analyzed hybrids are essentially composed of PBG and titania, implying that within the accuracy of TGA quantification, hydrolysis of the inorganic precursor prior to thermogravimetric analysis and removal of the reaction by-products during the thermal treatment at 110 °C are complete. It is therefore confirmed that the synthetic procedure adopted is a reliable and easy method to obtain hybrids with a controlled composition.

Table 3 summarizes the DSC results on hybrids with different compositions, while Fig. 6 shows representative DSC traces of the CX-20 series and of PBG for comparison. With increasing inorganic phase content in the hybrid, the glass transition shifts to higher temperature. This behaviour arises from the increasing number of Ti sites available for interaction with PBG chains that leads to a progressive increment of polymer chain constraints [46] and hence of T_g. At the same time the transition width broadens (see ΔT_g in Table 3), reflecting an increased relaxation time distribution due to a more heterogeneous chain length between Ti–polymer interaction points.

Table 3
Thermal properties of hybrids with different inorganic/organic phase compositions

Sample	Feed		Expected TiO_2/PBG wt% composition[a]	TGA			DSC[b]			
	TIPT/PBG (wt%)	HCl/Ti[c] (mol%)		Residue[d] (%)	T_g (°C)	ΔT_g (°C)	ΔCp (J/g °C)		T_m (°C)	ΔH_m (J/g)
							Exp	Calc[e]		
PBG	–	–	0/100	<0.5	−72	8	0.68	–	13	44
T25-20	25/75	20	9/91	11.2	−63	5	0.49	0.60	7	19
T50-20	50/50	20	22/78	22.1	−57	16	0.45	0.53	–	–
T75-20	75/25	20	46/54	44.5	−52	34	0.13	0.38	–	–
C25-20	25/75	20	9/91	9.9	−63	5	0.53	0.61	4	5
C50-20	50/50	20	22/78	21.1	−54	11	0.39	0.54	–	–
C60-20	60/40	20	30/70	29.1	−49	20	0.22	0.48	–	–
C75-20	75/25	20	46/54	43.0	−49	30	0.09	0.39	–	–

[a] Assuming completion of sol–gel reactions, i.e. hybrids composed of PBG and titania only.
[b] From the second heating scan after quench cooling.
[c] Molar ratio of acid vs. titanium (from titania precursor TIPT).
[d] Experimental solid residue at 600 °C.
[e] Based on actual PBG content in hybrids, evaluated from TGA residue.

It is worth noting that in the DSC curve of C25-20 (Fig. 6) the glass transition is followed by a small crystallization exotherm and by a subsequent melting endotherm. This observation suggests that the amount of titania in this hybrid (the actual titania content is 9.9 wt%, see Table 3) is not enough to fully prevent polymer crystallization. Conversely, in none of the analyzed hybrids with higher titania content is PBG able to crystallize. In C75-20 the interaction between the phases is so strong that almost no glass transition is detected, despite that in this hybrid the actual amount of polymer is 57 wt% (Table 3). It is worth noting that in all hybrids the experimental specific heat increment at the glass transition is lower than that expected based on the polymer content (compare ΔCp[Exp] with ΔCp[Calc]). A similar behaviour has been already reported for other hybrids [46,65] and confirms the strong interaction between organic and inorganic phases that inhibits polymer chain mobility.

All hybrids of the CX-20 and TX-20 series have been investigated by FT-IR spectroscopy. Fig. 7, as an example, shows results for CX-20 ceramers. Interestingly, the peak ascribed to Ti-transesterified carbonyl at 1535 cm^{-1}, that is almost undetectable in C25-20, increases with increasing titania content reaching in hybrid C75-20 around 30% of the unmodified carbonyl stretching band intensity (1740 cm^{-1}). As for the absorption at 610 cm^{-1}, associated with covalent bonding between titania and polymer, no such clear band intensification is observed owing to its overlap with other titania absorptions.

With the aim of confirming the suggested inter-phase bonding arising from transesterification reactions, XPS analyses have been carried out on three hybrid samples of the CX-20 series (C50-20, C60-20 and C75-20).

Fig. 8 shows, as an example, the XPS wide scan of C60-20 registered at a t.o.a. of 45°. The spectrum shows the presence, at the sample surface, of carbon (C_{1s} photoelectron peak centred at 285.0 eV), titanium (Ti_{2p} peak centred at 458.9), oxygen (O_{1s} peak centred at 532.5 eV) and silicon (Si_{2p} and Si_{2s} peaks centred at 101.7 and 155.0 eV, respectively). Silicon is attributed to a polydimethylsiloxane contamination that also contributes to the O_{1s} peak. Quantitative XPS analysis is carried out from narrow scans by the determination of core level peak areas obtained multiplying the experimental values by the appropriate sensitivity factor. Upon correction of the obtained values for the presence of siloxanes, relative atomic abundances of C, O and Ti are calculated (Table 4, experimental result). In addition, the actual composition of each hybrid (Table 3) is used to calculate the theoretical relative atomic abundances, also listed in Table 4. The comparison of theoretical and experimental atomic ratios clearly shows that at the surface the hybrid composition is different from the composition expected

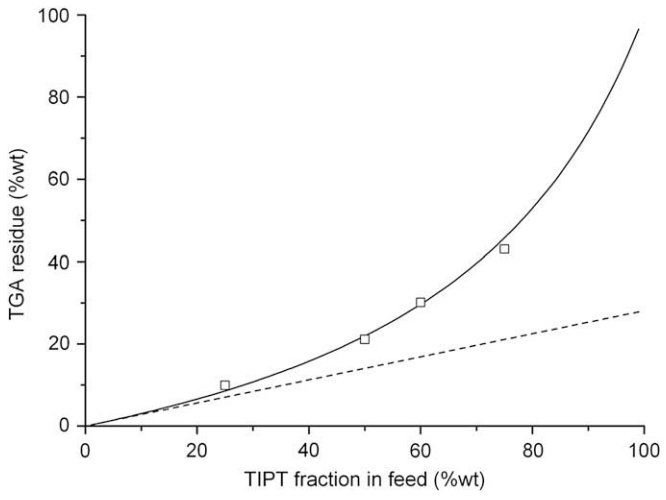

Fig. 5. TGA experimental solid residue of CX-20 hybrids plotted as a function of titania precursor (TIPT) in the feed (□). The drawn lines correspond to the titania solid residue calculated assuming that, before the TGA experiment, the sol–gel precursors have fully reacted (solid line) or are completely unreacted (broken line).

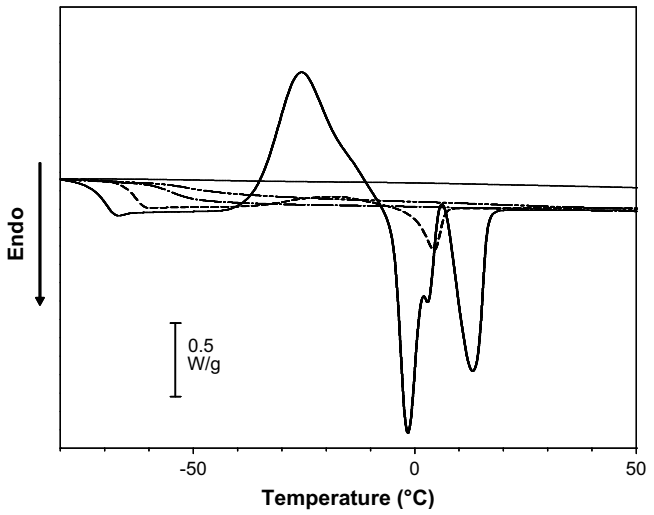

Fig. 6. DSC curves of PBG and of CY-20 hybrids: PBG (——), C25-20 (— —), C50-20 (— - —), C60-20 (— - - —) and C75-20 (·····).

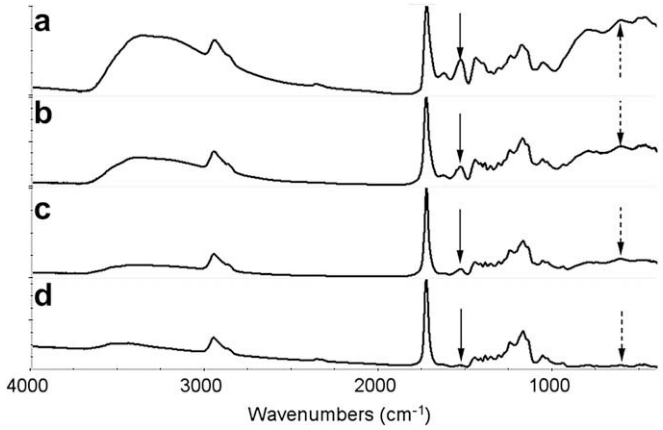

Fig. 7. Normalized FT-IR spectra of CX-20 hybrids: (a) C75-20, (b) C60-20, (c) C50-20 and (d) C25-20. Solid arrow: band at 1535 cm^{-1}; broken arrow: band at 610 cm^{-1}.

from the feed ratio, which is experimentally confirmed for the bulk of the sample by TGA results (Table 3). Since the photoelectron peak area is directly proportional to the number of atoms of the considered species, the fraction of titania (W) and of PBG (1-W) present at the surface of each sample has been then calculated, by the following relation:

$$\frac{A_{O1s}}{A_{Ti2p}} = \frac{\dfrac{2W}{PM_{TiO_2}} + \dfrac{22(1-W)}{PM_{PBG}}}{\dfrac{W}{PM_{TiO_2}}} \quad (3)$$

where A_{O1s} is the corrected O_{1s} peak area, A_{Ti2p} is the Ti_{2p} peak area, W is the surface weight percentage of titania and PM_{TiO_2} and PMPBG are the molecular weights of titania and PBG repeat unit respectively.

Calculation of PBG weight percentage at the surface shows that polymer concentration is higher than expected in all hybrids investigated (88% vs. 78% in C50-20; 76% vs. 70% in C60-20 and 62% vs. 54% in C75-20). Similar results of different composition in the bulk and at the surface were earlier obtained in other hybrid systems [66].

Resolution of characteristic core level shifts due to changes in the local chemical environment is one of the strong features of the XPS technique. In the present case, while Ti_{2p} and C_{1s} curve fitting elaboration does not show any detectable effect due to trans-esterification reactions, the elaboration made on the O_{1s} envelope allows us to draw some conclusion.

Fig. 8b shows, as an example, the curve fitting of the O_{1s} peak of hybrid C60-20 into three peaks labelled O_1, O_2 and O_3. The relative abundances and binding energy (BE) values of O_1, O_2 and O_3 are listed in Table 5 for the three analyzed hybrids. Based on the hybrid components (PBG and titania) and on literature results [67,68], the three O_{1s} component peaks can be associated with different oxygen species: O_1 with oxygen bound to Ti in TiO_2; O_2 with carbonyl oxygens C=O, O_3 with oxygen in C–O–C. Table 5 compares the experimental O_1, O_2 and O_3 values with theoretical values calculated from the actual surface composition (reported above). The latter calculated values are based on the assumption that no interaction between organic and inorganic phases exists in the hybrids.

Interestingly, in hybrids C60-20 and C75-20 a significant difference of experimental vs. calculated O_2 and O_3 contributions is observed (Table 5), with a strong increase of the former signal and an almost equivalent decrease of the latter signal. This behaviour is attributed to interaction between PBG and titania that alters oxygen binding energies. Since binding energy of O_2 is compatible with Ti–O–C oxygen type, the increase of O_2 signal and

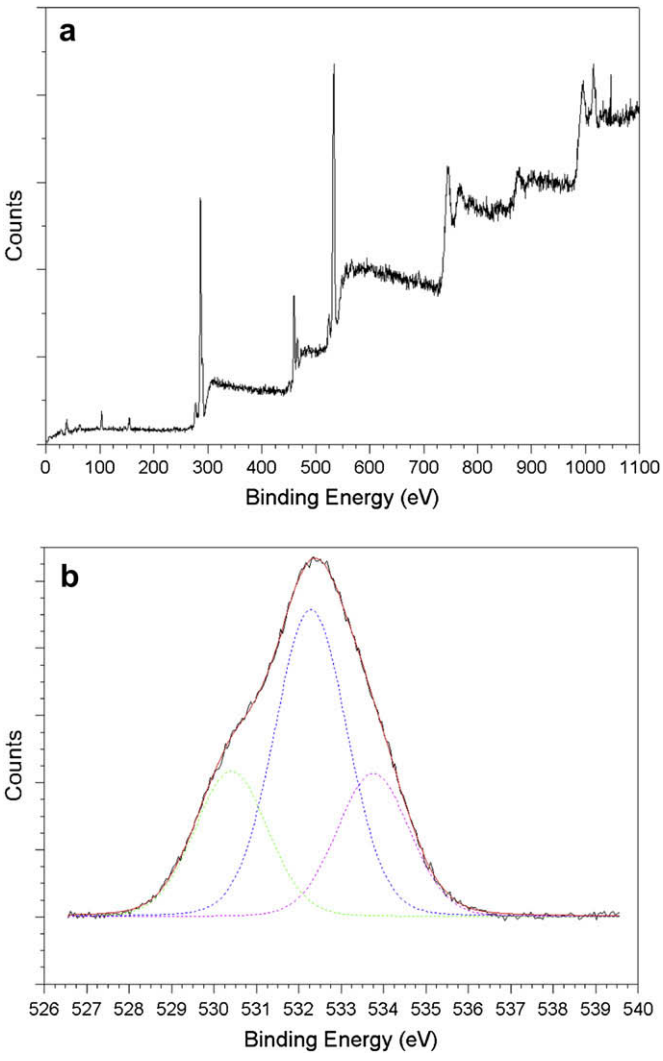

Fig. 8. Wide scan (a) and high resolution scan of O_{1s} peak (b) of C60-20 sample.

Table 4
Relative atomic abundances from XPS

Atomic ratios	C50-20		C60-20		C75-20	
	Exp.	Th[a]	Exp.	Th[a]	Exp.	Th[a]
O_{1s}/C_{1s}	0.39	0.63	0.46	0.67	0.57	0.95
O_{1s}/T_{2p}	14.3	8.12	7.85	6.09	4.86	4.04
Ti_{2p}/C_{1s}	0.027	0.078	0.058	0.11	0.12	0.23

[a] Calculated on the basis of the hybrid feed composition.

Table 5
Contribution of different oxygen types to O_{1s} signal, evaluated after deconvolution of the O_{1s} signal

O_{1s}	C50-20		C60-20		C75-20	
	Exp.[a] (%)	Calc.[b] (%)	Exp.[a] (%)	Calc.[b] (%)	Exp.[a] (%)	Calc.[b] (%)
O_1 (BE = 530.5 eV)	14.3	18.4	27.4	26.5	40.5	41.2
O_2 (BE = 532.4 eV)	47.4	44.5	45.6	40.1	38.8	32.1
O_3 (BE = 533.8 eV)	38.3	37.1	27.0	33.4	20.7	26.7

[a] Experimental results obtained from XPS analysis.
[b] Calculated on the basis of the actual composition of the analyzed layer assuming that the hybrid is made of PBG and titania without any interaction between the phases.

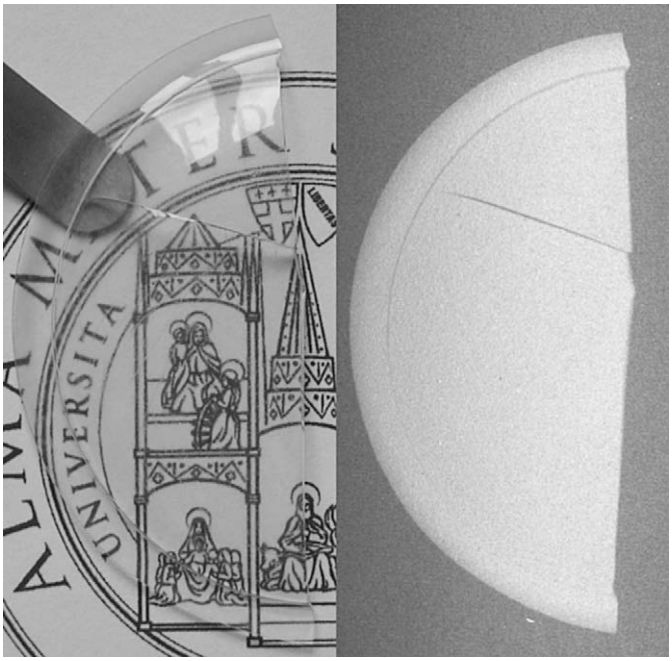

Fig. 9. Photographic (left) and radiographic (right) images of the same transparent and radiopaque hybrid sample C50-20.

contemporary decrease of O_3 (C–O–C oxygen) fully agree with the foregoing hypothesis of transesterification of the polyester chain by Ti atoms during hybrid formation (Scheme 2).

Hybrid C50-20 does not show such a clear trend possibly owing to too low an extent of transesterification in this sample to be significantly detected by XPS. In this context, the FT-IR spectra of Fig. 7 show that the intensity of the absorption at 1535 cm^{-1}, attributed to transesterified carbonyl stretching, is indeed much smaller in C50-20 than in C60-20 and C75-20.

A final characterization of the hybrids regards their interaction with electromagnetic radiation. In visible light, all investigated hybrids are transparent solids, irrespective of inorganic phase content. Given that amorphous PBG is a transparent polymer and that bulk amorphous titania is a white opaque material, this observation suggests that in the hybrids titania forms nanometric domains, according to the literature that locates the upper limit for transparency to visible light in multi-phase systems at 25–30 nm [8]. Another interesting property of these hybrids is their opacity to X-ray radiation. As shown in Fig. 9 for hybrid C50-20 taken as an example, a clearly contrasted image is obtained when the material is investigated using a mammographic equipment. As expected, radiopacity is seen to increase with titania content (pictures not shown). This peculiar property is currently under study, in view of a number of diversified potential applications [28].

4. Conclusions

This work shows that the synthesis of hybrid materials can be carried out by a simple and easy procedure. Application of a suitable curing treatment leads to hybrids constituted by the starting polyester and titania with a composition that can be precisely tuned by changing the feed of the sol–gel process.

The hybrids display thermal properties that depend on synthetic conditions, such as sol–gel solvent, acidity of the medium and content of inorganic precursor in the feed. The mentioned parameters influence phase interactions between the polyester and titania that mainly result from transesterification processes promoted by Ti that lead to organotitanium ester moieties. The presence of transesterification reaction products is confirmed by FT-IR and XPS results. The extent of the reaction strongly depends on the reaction solvent and on the presence of acid in the reaction mixture that, by affecting extent of transesterification, modify polymer chain mobility in the hybrid, as revealed by T_g increase and hindrance to crystallization.

All synthesized hybrids are transparent and provide highly contrasted radiographic images when analyzed in a mammographic equipment, thus paving the way to a number of possible applications of these materials in the fields of radiographic traceability and/or X-ray protection.

References

[1] Wilkes GL, Orler B, Huang H. Polym Prep 1985;26:300–1.
[2] Schmidt H. J Non-Cryst Solids 1985;73(1–3):681–91.
[3] Okada A, Usuki A. Mater Sci Eng C 1995;3(2):109–15.
[4] Gilman JW, Jackson CL, Morgan AB, Harris R, Manias E, Giannelis EP, et al. Chem Mater 2000;12(7):1866–73.
[5] Porter D, Metcalfe E, Thomas MJK. Fire Mater 2000;24(1):45–52.
[6] Armes SP. Polym News 1995;20:233–7.
[7] Godovski DY. Adv Polym Sci 1995;119:78–122.
[8] Caseri W. Macromol Rapid Commun 2000;21(11):705–22.
[9] Sanchez C, Julian B, Belleville P, Popall M. J Mater Chem 2005;15(35–36):3559–92.
[10] Huang H, Orler B, Wilkes GL. Macromolecules 1987;20(6):1322–30.
[11] Surivet F, Thanh ML, Pascault JP, Mai C. Macromolecules 1992;25(21):5742–51.
[12] Kohjiya S, Ochiai K, Yamashita S. J Non-Cryst Solids 1990;119(2):132–5.
[13] Huang H, Wilkes GL. Polym Bull 1987;18(5):455–62.
[14] Brennan AB, Wang B, Rodrigues DE, Wilkes GL. J Inorg Organomet Polym 1991;1(2):167–87.
[15] Brennan AB, Wilkes GL. Polymer 1991;32(4):733–9.
[16] Tian D, Dubois P, Jerome R. J Polym Sci Part A Polym Chem 1997;35(11):2295–305.
[17] Tian D, Dubois P, Jerome R. Polymer 1996;37(17):3983–7.
[18] Tian D, Blacher S, Dubois P, Jerome R. Polymer 1998;39(4):855–64.
[19] Saegusa T. J Macromol Sci A 1991;28(9):817–29.
[20] Noell JLW, Wilkes GL, Mohanty DK, McGrath JE. J Appl Polym Sci 1990;40(7–8):1177–94.
[21] Messori M, Toselli M, Pilati F, Fabbri E, Fabbri P, Pasquali L, et al. Polymer 2004;45:805–13.
[22] Kickelbick G. Prog Polym Sci 2003;28(1):83–114.
[23] Boettcher SW, Fan J, Tsung CK, Shi Q, Stucky GD. Acc Chem Res 2007;40(9):784–92.
[24] Soler-Illia GJDA, Scolan E, Louis A, Albouy PA, Sanchez C. New J Chem 2001;25(1):156–65.
[25] Livage J, Henry M, Sanchez C. Prog Solid State Chem 1988;18(4):259–341.
[26] Adams DM. Metal–ligand and related vibrations: a critical survey of the infrared and Raman spectra of metallic and organometallic compounds. New York: St. Martin's Press; 1968.
[27] Judeinstein P, Sanchez C. J Mater Chem 1996;6(4):511–25.
[28] Scandola M, Mazzocchetti L. PCT patent application IB2008/051640; 2008.
[29] Torchilin VP. Adv Drug Deliv Rev 2002;54(2):235–52.
[30] Kohn J, Zeltinger J. Exp Rev Med Dev 2005;2(6):667–71.
[31] Jayakrishnan A, Thanoo BC. Biomaterials 1990;11(7):477–81.
[32] Thanoo BC, Sunny MC, Jayakrishnan A. Biomaterials 1991;12(5):525–8.
[33] Thanoo BC, Sunny MC, Jayakrishnan A. J Appl Biomater 1991;2(2):67–72.
[34] Cabasso I, Smid J, Sahni SK. J Appl Polym Sci 1989;38(9):1653–66.
[35] Cabasso I, Smid J, Sahni SK. J Appl Polym Sci 1990;41(11–12):3025–42.
[36] Moszner N, Salz U, Klester AM, Rheinberger V. Angew Makromol Chem 1995;224(1):115–23.
[37] Horak D, Metalova M, Svec F. Biomaterials 1987;8(2):142–5.
[38] Jayakrishnan A, Thanoo BC, Rathinam K, Mohanty M. J Biomater Mater Res 1990;24(8):993–1004.
[39] Mottu F, Fenacht DA, Laurent A, Doelker E. Biomaterials 2002;23(1):121–31.
[40] James NR, Philip J, Jayakrishnan A. Biomaterials 2006;27(2):160–6.
[41] Dobson PJ. US patent 5,876,783; 1999.
[42] Sahagian R. US patent 7,077,837; 2006.
[43] Bearinger CR, Camilletti RC, Haluska LA, Michael KW, US patent 5,399,441; 1995.
[44] Blanchard J, In M, Schaudel B, Sanchez C. Eur J Inorg Chem 1998;8:1115–27.
[45] Takahashi R, Takenaka S, Sato S, Sodesawa T, Ogura K, Nakanishi K. J Chem Soc Faraday Trans 1998;94(20):3161–8.
[46] Mazzocchetti L, Sandri S, Scandola M, Bergia A, Zuccheri G. Biomacromolecules 2007;8(2):672–8.
[47] Ma H, Huang J, Qian Y. Inorg Chem Commun 2001;4(9):515–9.
[48] Zeynalov EB, Allen NS. Polym Degrad Stab 2006;91(4):931–9.
[49] Allen NS, Edge M, Ortega A, Sandoval G, Liauw CM, Verran J, et al. Polym Degrad Stab 2004;85(3):927–46.
[50] Yang J, Zhang S, Liu X, Cao A. Polym Degrad Stab 2003;81(1):1–7.
[51] Sanchez C, Ribot F. New J Chem 1994;18(10):1007–47.

[52] Blanchard J, Ribot F, Sanchez C, Bellot PV, Trokiner A. J Non-Cryst Solids 2000;265(1–2):83–97.
[53] Ceccorulli G, Zini E, Scandola M. Macromol Chem Phys 2006;207(10):864–9.
[54] Velasco MJ, Rubio F, Rubio J, Oteo JL. Thermochim Acta 1999;326(1–2):91–7.
[55] Li Y, White TJ, Lim SH. J Solid State Chem 2004;177:1372–81.
[56] Ge L, Xu M, Sun M, Fang H. Mater Res Bull 2006;41:1596–603.
[57] McDevitt NT, Baun WL. Spectrochim Acta 1964;20(5):799–808.
[58] Hampden-Smith MJ, Williams DS, Rheingold AL. Inorg Chem 1990;29(20):4076–81.
[59] Boettcher SW, Bartl MH, Hu JG, Stucky GD. J Am Chem Soc 2005;127(27): 9721–30.
[60] Nabavi M, Doeuff S, Sanchez C, Livage J. J Non-Cryst Solids 1990;121(1–3):31–4.
[61] Doeuff S, Henry M, Sanchez C, Livage J. J Non-Cryst Solids 1987;89(1–2):206–16.
[62] Chemin N, Rozes L, Chaneac C, Cassaignon S, Le Bourhis E, Jolivet JP, et al. Chem Mater 2008;20(14):4602–11.
[63] Kallala M, Sanchez C, Cabane B. Phys Rev E 1993;48(5):3692–704.
[64] Sayilkan F, Asilturk M, Sayilkan H, Onal Y, Akarsu M, Arpac E. Turk J Chem 2005;29:697–706.
[65] Mazzocchetti L, Scandola M, Amerio E, Malucelli G, Marano C. Macromol Chem Phys 2006;207(22):2103–11.
[66] Fabbri P, Messori M, Montecchi M, Nannarone S, Pasquali L, Pilati F, et al. Polymer 2006;47(4):1055–62.
[67] Li R, Nie K, Shen X, Wang S. Mater Lett 2007;61(6):1368–71.
[68] Yu DG, An JH, Ahn SD, Kang SR, Suh KS. Colloids Surf A 2005;266(1–3):62–7.